A Single-Strand Helical Motif Induced by Self-Assembly of $[Ag(TFP)]^+$ Moieties with Nitrate Anions − ^{31}P NMR Spectroscopic and X-ray Crystal Structure Characterization of the Complexes Involved in Equilibrium Reactions of Silver Salts and TFP Ligand

Fiorella Bachechi,[a] Alfredo Burini,*[b] Rossana Galassi,[b] Bianca Rosa Pietroni,[b] and Dania Tesei[b]

Keywords: P ligands / Silver / Helical structures / NMR spectroscopy / Equilibrium reactions

The ability of the ligand tris(2-furyl)phosphane (TFP) to coordinate Ag^I ions has been investigated. The molar ratio and the nature of the counterions used (NO_3^-; BF_4^-) affected the reaction. Moreover, equilibrium reactions were observed and the $[Ag(TFP)_n]^+$ (n = 1–4) species involved were identified by variable-temperature ^{31}P NMR spectroscopy. The $[Ag(TFP)_3]BF_4$ complex turned out to be the more labile species in solution and it disproportionates by means of an S_N2 mechanism to yield the complexes $[Ag(TFP)_2(H_2O)]BF_4$ (**3**) and $[Ag(TFP)_4]BF_4$ (**4**). Most of the compounds detected in solution were isolated and characterized in the solid state. The molecular structures of the complexes $[Ag(TFP)NO_3]$ (**1**), $[Ag(TFP)_3NO_3]$ (**2**), and $[Ag(TFP)_2(H_2O)]BF_4$ (**3**) were determined by X-ray crystal structure diffraction confirming the solution characterization data. In these structures the TFP ligand was always only bonded to the metal centre by the phosphorous atom. It is noteworthy to underline that the molecular structure of complex **1** consists of an infinite single-strand helix arising from the ability of the bridging nitrate anions to connect the $[Ag(TFP)]^+$ units. In the structure the nitrate anions are coordinated to the metal centres in unusual modes acting simultaneously as chelating and bridging ligands.

Introduction

There is a growing interest in investigating the role of tris(2-furyl)phosphane (TFP) in catalytic systems[1] and a comparative study between the function of Ph_3P or TFP in palladium(0)-catalysed reactions has been reported.[2] The coordinative ability of TFP with transition metal ions is not well known and few examples of TFP complexes have been structurally characterized, i.e. $[Fe_2(CO)_5(TFP)\mu\text{-}P(2\text{-furyl})_2]$[3] and $[Rh(CO)Cl_2(TFP)_2HgCl]$.[4]

As a part of an investigation on the chemistry of late transition metal ions coordinated to tertiary phosphane ligands containing heterocycles[5,6] we have studied the ability of TFP to coordinate Ag^I.

Silver(I) is one of the metal ions involved in the formation of helical compounds obtained by the self-assembly of silver salts and appropriate ligands.[7,8] Helical motifs are of great current interest in supramolecular chemistry,[9] organic synthesis,[10] material science[11] and metal complex drugs.[12] In general, the organization in helical structures derives from coded self-assembly of metal ions and simple ligands. Here we report the formation of a single-strand helical polymer governed by the nitrate counterion instead of the ancillary ligand coordinated to the metal centre. It is well known that even weakly coordinating anions have an effect on the coordination number and on the molecular structure of the transition metal complexes.[13] Thus, as far as silver(I) derivatives are concerned, different arrangements occur depending on the anion used. Tetranuclear cubane-like compounds $[AgPR_3X]_4$ (R = Et or Ph) were isolated when strongly coordinating anions (X^-) such as Cl^- or Br^- were used,[14,15] while mononuclear derivatives (i.e. $[Ag(PCy_3)_2NO_3]$, $[Ag(PCy_3)_2ClO_4]$) have been obtained by using weakly coordinating anions. In these last examples the silver ions are tetracoordinated and tricoordinated, respectively.[16] However, bicoordinated $[Ag(PR_3)_2]X$ compounds have also been structurally characterized {e.g.$[Ag\{P(CH_2CH_2CN)_3\}_2]NO_3$,[17] $[Ag\{P(mes)_3\}_2]PF_6$ (mes = $C_6H_2Me_3$-2,4,6)}.[18] Moreover, the NO_3^- counterion influences the ring conformations and the nuclearity of cyclic silver derivatives.[5,19]

Results and Discussion

The reactions of TFP phosphane ligand with silver(I) ions were affected by the molar ratio and by the nature of

---

[a] Istituto di Strutturistica Chimica "G. Giacomello" CNR, Roma, Italy
[b] Dipartimento di Scienze Chimiche Università di Camerino, Via S. Agostino 1, 62032 Camerino, Italy
Fax: (internat.) + 39-0737/637345
E-mail: alfredo.burini@unicam.it

the counterion used and equilibrium reactions were observed. With $AgNO_3$ as the silver salt and a 1:1 or 1:3 Ag/TFP molar ratio, the complexes $[Ag(TFP)NO_3]$ (**1**) and $[Ag(TFP)_3NO_3]$ (**2**) were isolated. Two other species: $[Ag(TFP)_2(H_2O)]BF_4$ (**3**) and $[Ag(TFP)_4]BF_4$ (**4**) were obtained treating TFP with $AgBF_4$ in THF solution and with either a 1:1 or 1:2 Ag/TFP molar ratio. Compound **4** is insoluble in THF and for this reason it was easily separated from the reaction mixture containing the more soluble compound **3**. However, compound **4** can be obtained in good yields when the right stoichiometry is used. The silver complexes synthesized and studied are represented in Scheme 1.

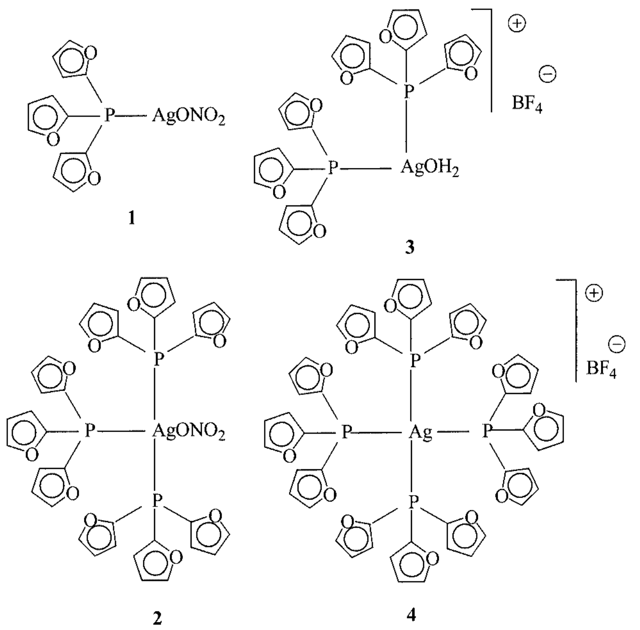

Scheme 1

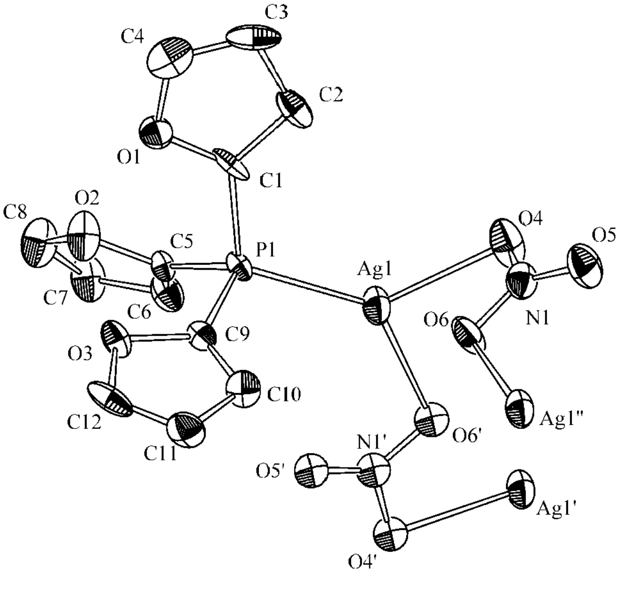

Figure 1. ORTEP plot of complex **1**, with the numbering schemes of the atoms; primed atoms are related by $P2_1$ symmetry with operators $-x$, $1/2 + y$, $1/2 - z$ for Ag(1) and $-x$, $-1/2 + y$, $1/2 - z$ for Ag(1′); thermal ellipsoids are shown at 40% probability levels

The molecular structures of compounds **1**−**3** were obtained by X-ray crystal structure determinations while the species present in solution were identified by variable-temperature ^{31}P NMR investigations.

Molecular and Crystal Structure of $[Ag(TFP)NO_3]$ (1)

The molecular structure of complex **1** with the atom numbering scheme is shown in Figure 1 and selected bond lengths and angles are listed in Table 1. In the solid-state structure of **1**, the silver ion is tetracoordinated. It is only linked to the potentially bidentate TFP ligand by the phosphorus atom; with a P(1)−Ag(1) distance of 2.366(3) Å. This length is short but still in the range of the P−Ag bond lengths (2.50−2.37 Å) found in other tertiary (phosphane)-silver derivatives.[16,17,20,21] The coordination sphere around the silver ion is completed by three oxygen atoms of the nitrate anion which is coordinated to the metal centre in quite a complex and unusual mode. In fact the nitrate group is bonded to the silver ion by O(4) [Ag(1)−O(4) = 2.38(1) Å] and O(6) [Ag(1)−O(6) = 2.63(1) Å] as an asymmetric chelating ligand. In addition, O(6′) [symmetry-related by a 2_1 screw axis to O(6)] is coordinated to the same silver ion Ag(1) [Ag(1)−O(6′) = 2.35(1) Å] and O(6) is coordinated to a silver ion Ag(1′′) {symmetry-related by a 2_1 screw axis to Ag(1)} [Ag(1′′)−O(6) = 2.35(1) Å]. In this way the nitrate anion acts as both a chelating and a bridging ligand. On the whole the Ag−O distances observed in compound **1** are similar to those found in $[Ag(PPh_3)NO_3]$ showing a zigzag chain of $AgNO_3$,[20] but they are shorter than those found in the related polymeric helical complex $[Ag(pydz)NO_3]$ (pydz = pyridazine).[7] However, the most relevant feature of the structure arises from the ability of the bridging nitrate anions to connect each $[Ag(TFP)]^+$ unit, forming an infinite single-strand helix, Figure 2. The silver ion also weakly interacts with O(5) of the 2_1-symmetry-related nitrate anion through the long 2.95(1) Å distance. Neglecting this last interaction, the coordination geometry around the metal centre can be described as a distorted tetrahedron with coordination angles P(1)−Ag(1)−O(4) = 128.1(3)°, P(1)−Ag(1)−O(6′) = 132.0(2)°, O(4)−Ag(1)−O(6′) = 99.9(3)°, and a bite angle of the nitrate group O(4)−Ag(1)−O(6) = 45.9(2)°. The crystal structure consists of the packing of single helices of both chiralities, coupled by centres of symmetry running along the *b* axis, Figure 3. The period of the helix is 7.37(1) Å and along the helix the Ag atoms lie at distances of 4.890(1) Å. The distance between Ag atoms, which belong to close centrosymmetric helices, is 5.642(2) Å. It is interesting to note that, from the particular arrangement of the helices, channels are formed in the centrosymmetric unit cell where small molecules could be trapped even though this has not yet been attempted.

Table 1. Selected bond lengths [Å] and angles [°] with e.s.d. values in parentheses

Complex **1**			
Ag(1)−P(1)	2.366(3)	P(1)−Ag(1)−O(4)	128.1(3)
Ag(1)−O(4)	2.38(1)	P(1)−Ag(1)−O(6′)	132.0(2)
Ag(1)−O(6)	2.63(1)	O(4)−Ag(1)−O(6′)	99.9(3)
Ag(1)−O(6′)	2.35(1)	Ag(1)−P(1)−C(1)	114.2(4)
P(1)−C(1)	1.78(1)	Ag(1)−P(1)−C(5)	114.7(4)
P(1)−C(5)	1.80(1)	Ag(1)−P(1)−C(9)	110.4(4)
P(1)−C(9)	1.79(1)	Ag(1)−O(4)−N(1)	101.1(7)
N(1)−O(4)	1.25(1)	Ag(1)−O(6)−N(1)	111.8(7)
N(1)−O(5)	1.24(1)	C(1)−P(1)−C(5)	105.2(5)
N(1)−O(6)	1.27(1)	C(1)−P(1)−C(9)	104.8(5)
		C(5)−P(1)−C(9)	106.8(5)
		O(4)−N(1)−O(5)	123(1)
		O(4)−N(1)−O(6)	119(1)
		O(5)−N(1)−O(6)	118(1)

Complex **3**			
Ag(1)−P(1)	2.425(3)	P(1)−Ag(1)−P(2)	131.2(1)
Ag(1)−P(2)	2.426(2)	P(1)−Ag(1)−O(7)	117.2(2)
Ag(1)−O(7)	2.36(1)	P(2)−Ag(1)−O(7)	111.0(2)
P(1)−C(1)	1.78(1)	Ag(1)−P(1)−C(1)	115.5(4)
P(1)−C(5)	1.79(1)	Ag(1)−P(1)−C(5)	111.4(4)
P(1)−C(9)	1.80(1)	Ag(1)−P(1)−C(9)	114.3(4)
P(2)−C(13)	1.79(1)	Ag(1)−P(2)−C(13)	115.7(3)
P(2)−C(17)	1.77(1)	Ag(1)−P(2)−C(17)	115.9(3)
P(2)−C(21)	1.80(1)	Ag(1)−P(2)−C(21)	110.0(4)
F(1)−B(1)	1.28(3)	C(1)−P(1)−C(5)	107.3(5)
F(2)−B(1)	1.33(2)	C(1)−P(1)−C(9)	104.6(5)
F(3)−B(1)	1.47(2)	C(5)−P(1)−C(9)	102.7(6)
F(4)−B(1)	1.33(3)	C(13)−P(2)−C(17)	102.7(5)
		C(13)−P(2)−C(21)	106.8(6)
		C(17)−P(2)−C(21)	104.7(5)
		F(2)−B(1)−F(1)	114(1)
		F(3)−B(1)−F(1)	105(1)
		F(3)−B(1)−F(2)	108(1)
		F(4)−B(1)−F(1)	110(1)
		F(4)−B(1)−F(2)	114(1)
		F(4)−B(1)−F(3)	102(1)

Complex **2**			
Ag(1)−P(1)	2.508(7)	P(1)−Ag(1)−P(2)	110.2(3)
Ag(1)−P(2)	2.512(7)	P(1)−Ag(1)−P(3)	113.9(2)
Ag(1)−P(3)	2.493(7)	P(1)−Ag(1)−O(11)	92(1)
Ag(1)−O(11)	2.71(3)	P(1)−Ag(1)−O(12)	130(1)
Ag(1)−O(12)	2.72(4)	P(2)−Ag(1)−P(3)	115.8(3)
P(1)−C(1)	1.74(2)	P(2)−Ag(1)−O(11)	99(1)
P(1)−C(5)	1.76(3)	P(2)−Ag(1)−O(12)	98(1)
P(1)−C(9)	1.82(2)	P(3)−Ag(1)−O(11)	122(1)
P(2)−C(13)	1.82(3)	P(3)−Ag(1)−O(12)	87(1)
P(2)−C(17)	1.78(3)	O(11)−Ag(1)−O(12)	42(1)
P(2)−C(21)	1.81(3)	Ag(1)−P(1)−C(1)	115(1)
P(3)−C(25)	1.80(3)	Ag(1)−P(1)−C(5)	119(1)
P(3)−C(29)	1.74(3)	Ag(1)−P(1)−C(9)	110(1)
P(3)−C(33)	1.80(3)	Ag(1)−P(2)−C(13)	110(1)
O(10)−N(1)	1.26(3)	Ag(1)−P(2)−C(17)	121(1)
O(11)−N(1)	1.09(3)	Ag(1)−P(2)−C(21)	116(1)
O(12)−N(1)	1.11(4)	Ag(1)−P(3)−C(25)	117(1)
		Ag(1)−P(3)−C(29)	111(1)
		Ag(1)−P(3)−C(33)	116(1)
		C(1)−P(1)−C(5)	102(1)
		C(1)−P(1)−C(9)	105(1)
		C(5)−P(1)−C(9)	103(1)
		C(13)−P(2)−C(17)	104(1)
		C(13)−P(2)−C(21)	103(1)
		C(17)−P(2)−C(21)	101(1)
		C(25)−P(3)−C(29)	104(1)
		C(25)−P(3)−C(33)	102(1)
		C(29)−P(3)−C(33)	105(1)
		P(1)−C(1)−O(1)	124(2)
		O(10)−N(1)−O(11)	122(4)
		O(10)−N(1)−O(12)	114(4)
		O(11)−N(1)−O(12)	124(4)

Molecular Structure of [Ag(TFP)$_3$NO$_3$] (2)

The molecular structure of complex **2**, with the atom numbering scheme, is shown in Figure 4 and selected bond lengths and angles are listed in Table 1. As far as we know, only one other example of [Ag(PR$_3$)$_3$X] complexes has been reported in the literature, namely [Ag(PPh$_3$)$_3$Cl],[22] showing a distorted tetrahedral geometry. Complex **2** contains mononuclear units in which the silver ion is five-coordinated by three phosphorus atoms of three TFP ligands and by two oxygen atoms belonging to the chelate nitrate ion. The geometry around the metal centre is a distorted square-base pyramid, where the silver ion lies 0.8098 Å out of the base formed by P(1), P(3), and two O atoms. The Ag−P bond lengths are longer [2.508(7), 2.512(7), 2.493(7) Å] than those found in complex **1** but slightly shorter than the Ag−P bond lengths found in [Ag(PPh$_3$)$_3$Cl] (2.52−2.56 Å). The nitrate ion is symmetrically bonded to the silver ion with a bite angle of 42(1)° and the Ag(1)−O(11) and Ag(1)−O(12) bond lengths are 2.71(3) Å and 2.72(4) Å, respectively.

Molecular Structure of [Ag(TFP)$_2$(OH$_2$)]BF$_4$ (3)

The molecular structure of complex **3**, with the atom numbering scheme, is shown in Figure 5 and selected bond lengths and angles are listed in Table 1.

The silver atom of the sixteen-electron complex **3** is tricoordinated with a distorted trigonal geometry. The metal ion is bonded to two TFP ligands by the P atoms and to one oxygen atom of a water molecule. The two Ag−P bond lengths are equivalent [2.425(3) Å and 2.426(2) Å]. They are very close to those found in [Ag{P(C$_6$H$_4$Me-*m*)$_3$}$_2$NO$_3$][17] (2.4128 Å), shorter than those found in [Ag(PPh$_3$)$_2$NO$_3$][23] and [Ag(PCy$_3$)$_2$NO$_3$] (ca. 2.44 Å),[16] but longer than those found in [Ag(PCy$_3$)$_2$ClO$_4$][16] [2.394(2), 2.393(3) Å] and in [Ag{P(CH$_2$CH$_2$CN)$_3$}$_2$]NO$_3$ [2.3832(9) Å].[17] The P(1)−Ag(1)−P(2) angle is 131.2(1)°. In the molecular structure of complex **3** an oxygen atom of a water molecule is coordinated to the metal ion [Ag(1)−O(7) 2.36(1) Å], revealing the poor coordinative ability of the oxygen atoms present in the furyl rings of the TFP ligand. Only one structure was recently reported,[4]

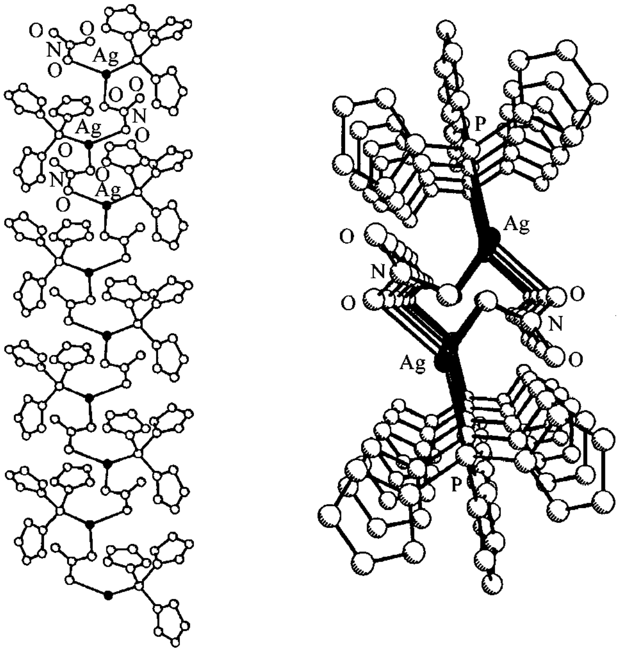

Figure 2. Complex **1**: (left) side view of the helical polymer chain extended along the crystallographic *b* axis with a helical period of 7.370(1) Å; the distance between Ag atoms is 4.891(1) Å; (right) top view along the axis of the polymer chain showing the twofold helical symmetry of the structure

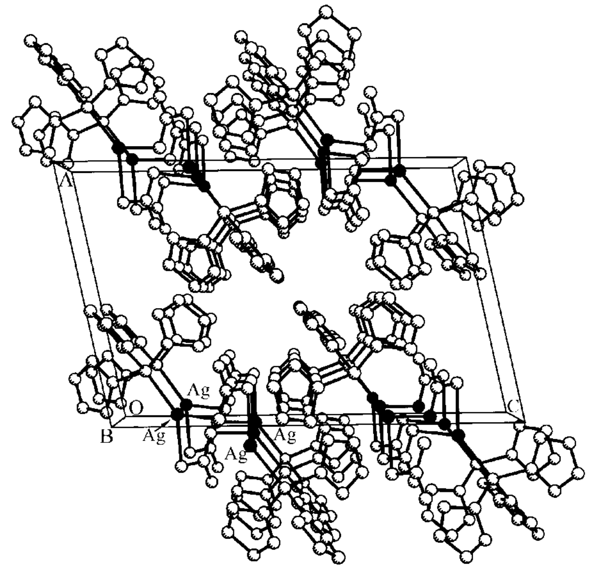

Figure 3. Unit cell content of complex **1** viewed down the *b* axis; adjacent chains are related by centres of symmetry

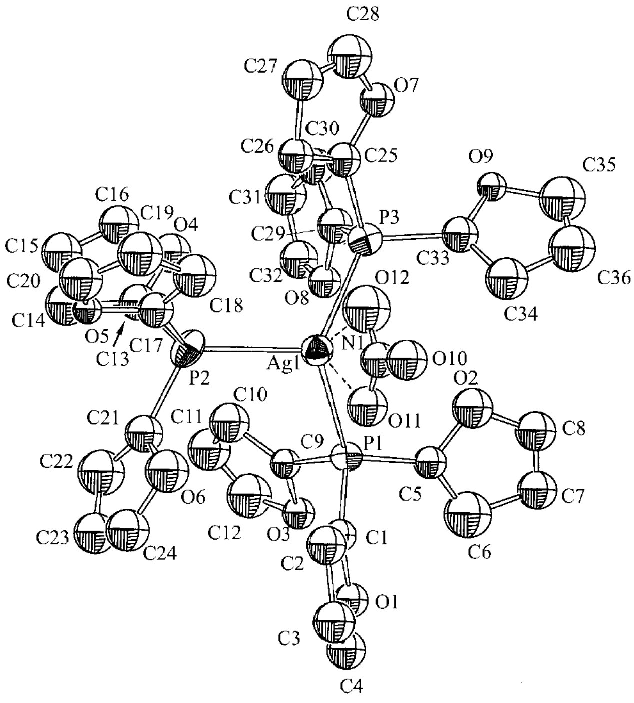

Figure 4. ORTEP plot of complex **2**, with the numbering schemes of the atoms; thermal ellipsoids are shown at 40% probability levels

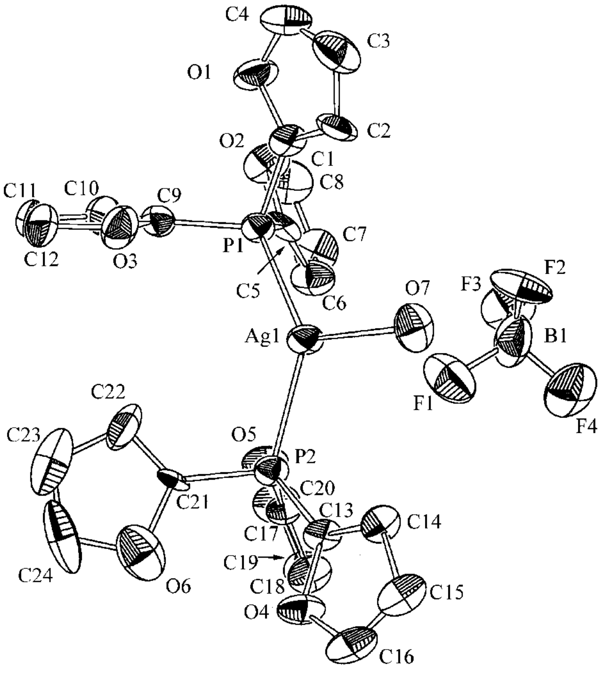

Figure 5. ORTEP plot of complex **3**, with the numbering schemes of the atoms; thermal ellipsoids are shown at 40% probability levels

where the furyl rings interact through the oxygen atoms to the metal centre {i.e. $[Rh(CO)Cl_2(TFP)_2HgCl]$; Hg−O distances 2.855(3) and 3.025(3) Å}. The BF_4^- anion is present in the structure of **3** as a counterion and weakly interacts with the water molecule [O(7)···F(1) 3.09 Å and O(7)···F(2) 2.93 Å].

^{31}P NMR Spectroscopic Investigation

The isolation in the solid state of several $[Ag(TFP)_nX]$ ($n = 1-4$; X = NO_3; BF_4) species highlights that equilibrium reactions could occur in solution. On the other hand silver(I) complexes are known to behave in this way when coordinated to labile monodentate ligands.[24,25] Thus to in-

Table 2. $^{31}P\{^1H\}$ NMR spectroscopic data of the Ag(TFP) species detected in $CDCl_3$ solution

Compound	δ (296 K)	δ (218 K)	$^1J(^{31}P,^{107}Ag)$ [Hz] (218 K)	$^1J(^{31}P,^{109}Ag)$ [Hz] (218 K)
TFP	−77.37 (s)			
TFP=O	−11.14 (s)	−10.00 (s)		
$[Ag(TFP)NO_3]$ (**1**)	−56.30 (m, br.)	−63.30 (dd)	699	803
$[Ag(TFP)_2NO_3]$		−62.40 (dd)	467	537
$[Ag(TFP)_2(OH_2)]BF_4$ (**3**)	−55.77 (s, br.)	−60.08 (dd)[a]	519[a]	573[a]
$[Ag(TFP)_3]BF_4$		−58.42 (d, br.)[a]		
$[Ag(TFP)_4]BF_4$ (**4**)	−57.48 (s, br.)	−56.74 (dd)	246	285

[a] The spectrum was recorded at 193 K in $CDCl_3 + CF_2Br_2$ solution.

vestigate this aspect, variable-temperature ^{31}P NMR spectra were recorded on compounds **1**−**4**, Table 2.

Compound **1**, that has a polymeric nature in the solid state, probably exists as a monomeric unit in solution. This hypothesis is reasonable because the silver ions forming the helical structure are held together only by bridging nitrate groups that, in solution, can easily break the bridging bonds. On the other hand the loss of the polymeric nature of compound **1** is underlined by the presence of the equilibrium reaction to be discussed.

Owing to rapid intermolecular ligand exchange in $CDCl_3$ solution, the ^{31}P NMR spectrum of compound **1**, recorded at 296 K, shows a broad signal at δ = −56.30 that is shifted to lower fields with respect to the free TFP ligand (δ = −77.37). By cooling the solution at 218 K the signal sharpened into two doublets of doublets, Figure 6. Each doublet of doublets is due to the spin-spin coupling of the phosphorus atom of the ligand with the two magnetically active isotopes of the silver ion (^{107}Ag spin 1/2, natural abundance 51.82%; ^{109}Ag spin 1/2, natural abundance 48.18%). Taking into consideration that the coupling constants decrease when the number of the phosphane ligands coordinated to the silver ion increase, the two AB systems of the ^{31}P NMR spectrum were assigned to $[Ag(TFP)NO_3]$ (**1**) and $[Ag(TFP)_2NO_3]$ complexes. Thus the signal centred at δ = −63.30, $^1J(^{31}P,^{107}Ag)$ = 699 Hz and $^1J(^{31}P,^{109}Ag)$ = 803 Hz was assigned to compound **1**; while the doublet of doublets centred at δ = −62.40, $^1J(^{31}P,^{107}Ag)$ = 467 Hz and $^1J(^{31}P,^{109}Ag)$ = 537 Hz was attributed to the compound $[Ag(TFP)_2NO_3]$. The values of the coupling constants observed for both complexes are in perfect agreement with the expected magnetogyric ratios. This interpretation of the spectrum was confirmed by the isolation in the solid state of complex $[Ag(TFP)_2(OH_2)]BF_4$ (**3**) showing the chemical shift of the ^{31}P nucleus and the Ag,P coupling constants similar to that observed for the species $[Ag(TFP)_2NO_3]$ identified only in solution (see discussion reported below). From the data the following equilibrium reaction seems to occur in solution:

$2\,[Ag(TFP)NO_3] \rightleftarrows [Ag(TFP)_2NO_3] + AgNO_3$.

The ^{31}P NMR spectrum of the analytically pure sample of $[Ag(TFP)_3NO_3]$ (**2**) recorded in $CDCl_3$ solution at 296 K shows two signals, a sharp one at δ = −11.14 and a broad one at δ = −57.00. By cooling the solution to 218 K the phosphorus, silver spin-spin coupling is solved, Figure 7. The spectrum shows a singlet at δ = −10.00 assigned to tris(2-furyl)phosphane oxide and a doublet of doublets at δ = −62.40 [$^1J(^{31}P,^{107}Ag)$ = 467 Hz and $^1J(^{31}P,^{109}Ag)$ = 537 Hz] that, as reported above, belongs to the $[Ag(TFP)_2NO_3]$ complex. Thus, we can conclude that when the complex $[Ag(TFP)_3NO_3]$ is dissolved in the presence of atmospheric oxygen, it gives rise to a dissociative process, and a fast oxidation of the free TFP ligand occurs. The lability of complex **2** in solution results in low yields of this compound.

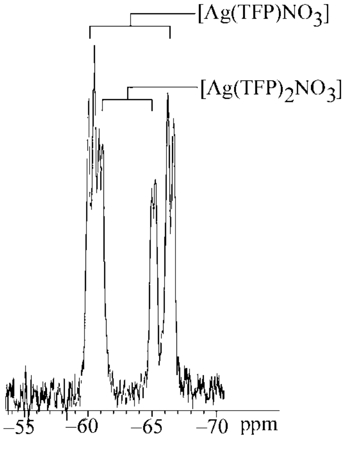

Figure 6. ^{31}P NMR spectrum recorded at 218 K; the signal centred at δ = −63.30 belongs to the complex $[Ag(TFP)NO_3]$ (**1**) while the doublet of doublets centred at δ = −62.40, was attributed to the compound $[Ag(TFP)_2NO_3]$

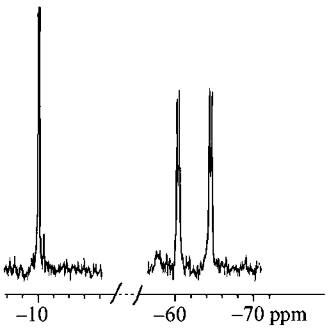

Figure 7. ^{31}P NMR spectrum recorded at 218 K; the species $[Ag(TFP)_3NO_3]$ decomposed in $CDCl_3$ solution to give tris-(2-furyl)phosphane oxide and $[Ag(TFP)_2NO_3]$ signals at δ = −10.00 and −62.40, respectively

Differing from the compounds discussed above, complexes **3** and **4** were simultaneously obtained by the same reaction mixture (see Exp. Sect.). This could be explained taking into consideration, the hypothesis, that in the first step the labile complex [Ag(TFP)$_3$]BF$_4$ is formed, which disproportionates to give the bis and tetrakis complexes **3** and **4**, respectively. The plausible S$_N$2 mechanism is reported in Scheme 2. The presence of water molecules in the reaction mixture could be due to the highly hygroscopic AgBF$_4$ salt used in the reaction.

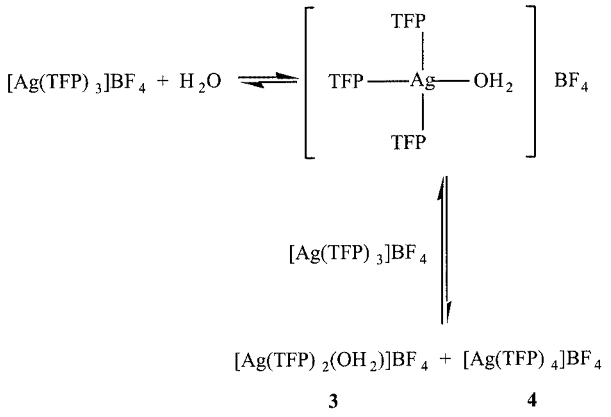

Scheme 2

The proposed mechanism and the equilibrium reactions involved were confirmed by the ^{31}P NMR spectrum obtained after dissolving an analytical sample of **3** in CDCl$_3$. The spectrum recorded at 193 K is shown in Figure 8. It consists of three systems centred at $\delta = -60.08$, -58.42, and -56.74. On the basis of the coupling constants the doublet of doublets at $\delta = -60.08$ [$^1J(^{31}P,^{107}Ag) = 519$ Hz and $^1J(^{31}P,^{109}Ag) = 573$ Hz] was assigned to complex **3**, while the doublet of doublets at $\delta = -56.74$ [$^1J(^{31}P,^{107}Ag) = 246$ Hz and $^1J(^{31}P,^{109}Ag) = 285$ Hz] was attributed to the tetrakis complex **4**. The different chemical shift (ca. 2 ppm) of **3** compared to that observed in the analogous [Ag(TFP)$_2$NO$_3$] complex, could be due to the influence of the different anions of these two complexes or to the water molecule presents in the coordination sphere of **3**. The last signal of the spectrum centred at $\delta = -58.42$ consists of an unresolved doublet of doublets belonging to the species [Ag(TFP)$_3$]BF$_4$, that being labile, gives quite a broad signal at low temperatures. The complex was not isolated in the solid state; thus, it seems to be only a transient species in solution.

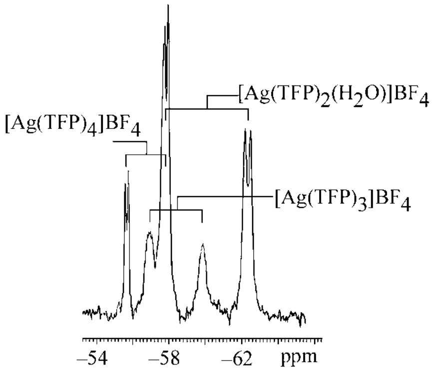

Figure 8. ^{31}P NMR spectrum recorded at 193 K; the three systems centred at $\delta = -60.08$, -58.42, and -56.74 were assigned to the complexes [Ag(TFP)$_2$(H$_2$O)]BF$_4$ (**3**) [Ag(TFP)$_3$]BF$_4$ and [Ag(TFP)$_4$]BF$_4$ (**4**), respectively

A successful attempt to obtain complex **4** in good yield was done treating the TFP ligand and AgBF$_4$ in a 4:1 molar ratio; from this reaction mixture only a small amount of complex **3** was obtained. The ^{31}P NMR spectrum of an analytical sample of **4** recorded at 296 K shows a sharpened signal at $\delta = -57.48$ that is solved in a doublet of doublets at 218 K, the chemical shifts and the coupling constants observed were the same as those reported above. The ligand lability of complex **4** is confirmed by the loss of the Ag,P coupling at temperatures above ca. 218 K.

Experimental Section

General: Elemental analyses were carried out with a Carlo Erba 1106 elemental microanalyser. ^{1}H and ^{31}P NMR spectra were performed in CDCl$_3$ solution with Varian VXR-300 spectrometers. Referencing is relative to TMS (^{1}H) and 85% H$_3$PO$_4$ (^{31}P). Variable-temperature ^{31}P NMR spectroscopic experiments were recorded over the temperature range 193−296 K. The reactions were carried out in the darkness at room temperature under nitrogen and with purified solvents.

Reaction of TFP with AgNO$_3$ (1:1 Molar Ratio); Compound 1: To a solution of TFP (0.10 g; 0.43 mmol) in THF (6 mL), crystalline AgNO$_3$ (0.074 g; 0.43 mmol) was added. Methanol (4 mL) was added to the reaction mixture to solubilize the silver salt. After 2 h, the solution was concentrated to dryness. The crude product was crystallized by slow diffusion of hexane into a dichloromethane solution. Colourless needles of **1** suitable for an X-ray crystal structure determination were formed after a few days (yield 0.104 g, 60%). C$_{12}$H$_9$AgNO$_6$P (**1**) (402.0): calcd. C 35.85, H 2.26, N 3.48; found C 36.25, H 2.35, N 3.26. ^{1}H NMR (CDCl$_3$; 296 K): $\delta = 6.51$ (m, 3 H), 7.11 (m, 3 H), 7.74 (m, 3 H). ^{31}P{^{1}H} NMR (CDCl$_3$; 296 K): $\delta = -56.30$ (m, br.)

Reaction of TFP with AgNO$_3$ (3:1 Molar Ratio); Compound 2: To a solution of TFP (0.10 g; 0.43 mmol) in THF (6 mL), crystalline AgNO$_3$ (0.024 g; 0.14 mmol) and methanol (4 mL) were added. After 2 h, the solution was concentrated to dryness. The solid obtained was dissolved in the minimum amount of dichloromethane and, after filtration, the solution was cooled to 4 °C. Colourless crystals of **2** suitable for an X-ray crystal structure determination grew overnight (yield 0.030 g; 30%). C$_{36}$H$_{27}$AgNO$_{12}$P$_3$ (**2**) (866.4): calcd. C 49.91, H 3.14, N 1.62; found C 49.74, H 3.24, N 1.65. ^{1}H NMR (CDCl$_3$; 296 K): $\delta = 6.47$ (m, 9 H), 7.13 (m, 9 H), 7.70 (s, 9 H). ^{31}P{^{1}H} NMR (CDCl$_3$; 296 K): $\delta = -11.14$ (s), -57.00 (m, br.)

Reaction of TFP with AgBF$_4$ (2:1 Molar Ratio); Compounds 3 and 4: To a solution of TFP (0.15 g; 0.65 mmol) in THF (6 mL), AgBF$_4$ (0.068 g; 0.32 mmol) was added. A cloudy solution was immediately obtained. After 1 h, the white precipitate was separated from the supernatant by centrifugation, to give the analytical sample of **4** (yield 0.085 g; 47%, calculated respect to the amount of the TFP ligand used). The solution was concentrated to dryness and the crude product obtained was dissolved in hot chloroform. Crystals of **3** suitable for an X-ray crystal structure determination (yield 0.089 g; 40%, calculated with respect to the amount of the TFP ligand used) were obtained by cooling the chloroform solution to 4 °C. With TFP and $AgBF_4$ in a 1:1 molar ratio, compounds **3** and **4** were both obtained. $C_{24}H_{20}AgBF_4O_7P_2$ (**3**) (677.0): calcd. C 42.58, H 2.98; found C 42.89, H 2.75. ^1H NMR ($CDCl_3$; 296 K): $\delta = 1.85$ (s, 2 H), 6.48 (m, 6 H), 7.19 (m, 6 H), 7.68 (s, 6 H). $^{31}P\{^1H\}$ NMR ($CDCl_3$; 296 K): $\delta = -55.77$ (s, br.). $C_{48}H_{36}AgBF_4O_{12}P_4$ (**4**) (1123.4): calcd. C 51.32, H 3.23; found C 51.40, H 3.11. ^1H NMR ($CDCl_3$; 296 K): $\delta = 6.36$ (m, 12 H), 6.74 (m, 12 H), 7.38 (s, br 12 H). $^{31}P\{^1H\}$ NMR ($CDCl_3$; 296 K): $\delta = -57.48$ (s, br.)

Reaction of TFP with $AgBF_4$ (4:1 Molar Ratio); Compound 4: To a solution of TFP (0.15 g; 0.65 mmol) in THF (6 mL), $AgBF_4$ (0.031 g; 0.16 mmol) was added. The cloudy solution was stirred for 0.5 h and a white precipitated of **4** formed (0.15 g; yield 84%). The supernatant, separated by centrifugation from the precipitate, was concentrated to dryness. The oily crude product was washed with hexane and then crystallized from $CHCl_3$; a small amount of **3** was recovered. $C_{48}H_{36}AgBF_4O_{12}P_4$ (**4**) (1123.4): calcd. C 51.32, H 3.23; found C 51.18, H 3.07. ^1H NMR ($CDCl_3$; 296 K): $\delta = 6.36$ (m, 12 H), 6.74 (m, 12 H), 7.38 (s, br., 12 H). $^{31}P\{^1H\}$ NMR ($CDCl_3$; 296 K): $\delta = -57.48$ (s, br.)

X-ray Crystal Structure Analyses of 1, 2, and 3: X-ray diffraction data of single crystals of the three complexes were collected with a Rigaku AFC5R diffractometer with graphite-monochromated Cu-K_α radiation and a 12-kV rotating anode generator. Intensity data were collected by the ω-2θ technique to a maximum 2θ value of about 124°. Corrections for Lorentz polarisation and absorption were applied to the data of the three compounds. A linear correction factor was applied to the data of **2** to account for the intensity decay of −61% detected in the intensities of the standard reflections. The structures were solved by Patterson methods and subsequent Fourier analyses and refined by the full-matrix least-squares method with anisotropic thermal parameters for all non-hydrogen atoms of **1** and **3** and for the heavier atoms of **2**, while the carbon and oxygen atoms of the furyl groups were refined isotropically. The hydrogen atoms were included at calculated positions and not refined for the three compounds. Crystal parameters and structure determination data are given in Table 3. Atomic scattering factors and anomalous dispersion terms were taken from the International Tables.[26] All calculations were performed by using the TEXAN crystallographic software package.[27] CCDC-164610 (**1**), -164611 (**2**) and -164612 (**3**) contain the supplementary crystallographic data for this paper. These data can be obtained free of charge at www.ccdc.cam.ac.uk/conts/retrieving.html or from the

Table 3. Crystal data

Compound	1	2	3
Empirical formula	$C_{12}H_9AgNO_6P$	$C_{36}H_{27}AgNO_{12}P_3$	$C_{24}H_{18}AgBF_4O_6P_2$
Molecular mass	402.05	866.40	675.02
Crystal size [mm]	0.20 × 0.30 × 0.60	0.25 × 0.50 × 0.70	0.10 × 0.20 × 0.30
Crystal system	monoclinic	orthorhombic	triclinic
a [Å]	11.274(1)	18.291(4)	13.009(5)
b [Å]	7.370(1)	24.052(5)	10.789(3)
c [Å]	17.106(2)	17.027(6)	10.839(4)
α [°]	90	90	68.50(3)
β [°]	101.58(1)	90	80.22(3)
γ [°]	90	90	75.00(4)
V [$Å^3$]	1392.3(4)	7491(3)	1362(1)
Space group	$P2_1/c$ (#14)	$Pbca$ (#61)	$P\bar{1}$ (#2)
Z	4	8	2
$D_{calcd.}$ [$g \cdot cm^{-3}$]	1.918	1.537	1.646
$F(000)$	792	3504	672
μ(Cu-K_α) [cm^{-1}]	132.08	61.59	7.80
Scan type	ω-2θ	ω-2θ	ω-2θ
Scan rate [$° \cdot min^{-1}$]	16.00 (3 rescans)	16.00 (3 rescans)	16.00 (3 rescans)
Scan width [°]	0.94 + 0.30 tanθ	1.10 + 0.30 tanθ	1.37 + 0.30 tanθ
$2\theta_{max.}$ [°]	124.20	124.10	124.2
No. measured reflections			
total	4931	6518	4516
unique	4692	6202	4297
corrections	Lorentz polarisation	Lorentz polarisation	Lorentz polarisation
Abs. trans. factors	0.73−1.00	0.53−1.00	0.30−1.00
Decay	−61%		
Refinement	full matrix	full matrix	full matrix
Function minimised	$w(\lvert F_o\rvert - \lvert F_c\rvert)^2$	$w(\lvert F_o\rvert - \lvert F_c\rvert)^2$	$w(\lvert F_o\rvert - \lvert F_c\rvert)^2$
Least-squares weights	$4F_o^2/\sigma^2(F_o^2)$	$4F_o^2/\sigma^2(F_o^2)$	$4F_o^2/\sigma^2(F_o^2)$
p factor	0.03	0.03	0.03
No. observations [$I > 3\sigma(I)$]	1453	1538	2569
No. variables	190	233	353
Reflection/parameter ratio	7.7	6.60	7.3
Residuals: R; Rw	0.062; 0.077	0.077; 0.087	0.071; 0.085
Goodness of fit indicator	0.10	0.55	0.75
Max shift/error	0.59	0.11	0.80
Max peak diff. map [$e \cdot Å^{-3}$]	0.61	0.37	0.70
Min peak diff. map [$e \cdot Å^{-3}$]	−1.32	−0.26	−1.21

Cambridge Crystallographic Data Centre, 12, Union Road, Cambridge CB2 1EZ, UK [Fax: (internat.) + 44-1223/336-033; E-mail: deposit@ccdc.cam.ac.uk].

Acknowledgments

This work was supported by grants from University of Camerino and CNR (Roma).

---

[1] V. Farina, S. R. Baker, D. A. Benigni, S. I. Hauck, C. Sapino, Jr., *J. Org. Chem.* **1990**, *55*, 5833.

[2] C. Amatore, A. Jutand, G. Meyer, H. Atmani, F. Khalil, F. O. Chahdi, *Organometallics* **1998**, *17*, 2958 −and references therein).

[3] C. Santelli-Rouvier, C. Coin, L. Toupet, M. Santelli, *J. Organomet. Chem.* **1995**, *495*, 91.

[4] S.-M. Kuang, F. Xue, T. C. W. Mak, Z.-Z. Zhang, *Inorg. Chim. Acta* **1999**, *284*, 119.

[5] [5a] F. Bachechi, A. Burini, R. Galassi, A. Macchioni, B. R. Pietroni, F. Ziarelli, C. Zuccaccia, *J. Organomet. Chem.* **2000**, *593−594*, 392. [5b] T. S. A. Hor, S. P. Neo, C. S. Tan, T. C. W. Mak, K. W. P. Leung, R-J. Wang, *Inorg. Chem.* **1992**, *31*, 4510.

[6] C. Tejel, R. Bravi, M. A. Ciriano, L. A. Oro, M. Bordonaba, C. Graiff, A. Tiripicchio, A. Burini, *Organometallics* **2000**, *19*, 3115.

[7] [7a] L. Carlucci, G. Ciani, D. W. v. Gudenberg, D. M. Proserpio, *Inorg. Chem.* **1997**, *36*, 3812. [7b] L. Carlucci, G. Ciani, D. M. Proserpio, A. Sironi, *Inorg. Chem.* **1998**, *37*, 5941. [7c] Y. Fu, J. Sum, Q. Li, Y. Chen, W. Dai, D. Wang, T. C. W. Mak, W. Tang, H. Hu, *J. Chem. Soc., Dalton Trans.* **1996**, 2309.

[8] C. A. Hester, R. G. Baughman, H. L. Collier, *Polyhedron* **1997**, *16*, 2893.

[9] [9a] K. D. Karlin (Ed.), *Progress in Inorganic Chemistry*, John Wiley & Sons, Inc., New York, **1994**, vol. 42. [9b] J. M. Lehn, *Angew. Chem. Int. Ed. Engl.* **1990**, *29*, 1304. [9c] W. Zarges, J. Hall, J. M. Lehn, C. Bolm, *Helv. Chim. Acta* **1991**, *74*, 1843.

[10] [10a] E. J. Corey, C. L. Cymin, M. C. Noe, *Tetrahedron Lett.* **1994**, *35*, 69. [10b] K. Maruoka, N. Murase, H. Yamamoto, *J. Org. Chem.* **1993**, *58*, 2938.

[11] C. Chen, K. S. Suslick, *Coord. Chem. Rev.* **1993**, *128*, 293 and references therein.

[12] K. Nomiya, S. Takahashi, R. Noguchi, S. Nemoto, T. Takayama, M. Oda, *Inorg. Chem.* **2000**, *39*, 3301.

[13] M. Dartiguenave, Y. Dartiguenave, A. Mari, A. Guitard, M. J. Olivier, A. L. Beauchamp, *Can. J. Chem.* **1988**, *66*, 2386.

[14] B.-K. Teo, J. C. Calabrese, *Inorg. Chem.* **1976**, *15*, 2467.

[15] M. R. Churchill, J. Donahue, F. J. Rotella, *Inorg. Chem.* **1976**, *15*, 2752.

[16] M. Camalli, F. Caruso, *Inorg. Chim. Acta* **1988**, *144*, 205.

[17] C. W. Liu, H. Pan, J. P. Fackler, Jr., G. Wu, E. Wasylishen, M. Shang, *J. Chem. Soc., Dalton Trans.* **1995**, 3691.

[18] E. C. Alyea, G. Ferguson, A. Smogyvari, *Inorg. Chem.* **1982**, *21*, 1369.

[19] D. M. Ho, R. Bau, *Inorg. Chem.* **1983**, *22*, 4073.

[20] R. A. Stein, C. Knobler, *Inorg. Chem.* **1977**, *16*, 242 and references therein.

[21] G. A. Ardizzoia, G. La Monica, A. Maspero, M. Moret, N. Masciocchi, *Inorg. Chem.* **1997**, *36*, 2321.

[22] A. Cassel, *Acta Crystallogr., Sect. B* **1981**, *37*, 229.

[23] P. F. Barron, J. C. Dyason, P. C. Healy, L. M. Engelhardt, W. Skelton, B. A. H. White, *J. Chem. Soc., Dalton Trans.* **1986**, 1965.

[24] A. Del Zotto, P. Di Bernardo, M. Tolazzi, G. Tomat, P. Zanonato, *Chem. Soc., Dalton Trans.* **1993**, 3009.

[25] E. L. Muetterties, C. W. Alegranti, *J. Am. Chem. Soc.* **1972**, *94*, 6386 [exhaustive article regarding ^{31}P NMR investigation of silver(I)-phosphane and -phosphite complexes].

[26] *International Tables for X-ray Crystallography*, vol. IV, Kynoch Press, Birmingham, UK, **1974**.

[27] *TEXSAN-TEXRAY*, Structure Analysis Package, Molecular Structure Corporation, **1985**.

Received August 1, 2001
[I01284]